This is a repository copy of *A circuit-theoretic approach to the design of quadruple-mode broadband microstrip patch antennas* .

White Rose Research Online URL for this paper:
http://eprints.whiterose.ac.uk/3796/

Article:

A Circuit-Theoretic Approach to the Design of Quadruple-Mode Broadband Microstrip Patch Antennas

Alaa I. Abunjaileh, *Student Member, IEEE*, Ian C. Hunter, *Fellow, IEEE*, and Andrew H. Kemp

Abstract—A novel method for the design of broadband patch antennas is described. The approach taken is to broadside couple two dual-mode patch antennas, resulting in a quad resonance antenna. The equivalent circuit of the antenna is similar to that of microwave filters, thus filter design techniques maybe employed to synthesize the antenna to obtain maximum return-loss bandwidth. This is the first time an increase in the bandwidth is achieved on a relatively thin substrate antenna as a result of coupling four resonant modes using two stacked circular microstrip patches. Electromagnetic simulation and measured results demonstrate bandwidth improvement of over four times that of a single-mode design.

Index Terms—Microstrip antennas, microstrip filters, microwave filters, multifrequency antenna, resonators.

I. INTRODUCTION

CIRCULAR microstrip patch antennas are widely used in wireless applications for their well-known advantages of ease of construction, strong mechanical structure, low profile, and low cost. However, the major problem of this type of antenna is their inherent narrow bandwidth [1]. Multilayer microstrip antennas were proposed in the 1970s [2]–[4], where two- or three-layer stacked microstrip patches provided a considerably wider bandwidth due to the multiresonator effect [1], [5], [7], [8]. Since then, more research has been carried out, reporting various methods of stacked resonators [5], [6]. Structures such as circular, square, and triangular microstrip patch antennas can support two orthogonal resonant modes or two polarizations [9]. In previous papers by Abunjaileh *et al.* [10] and Hunter [11], it was shown that it is possible to design a dual-polarized patch antenna as if it was a dual-mode filter, which significantly improves the bandwidth. In this paper, a new stacked two layer antenna is presented from theory that has been extended to the design of a quadruple-mode antenna (this is described in Section II). Electromagnetic simulations and measured results presented in Section III show over four times bandwidth enhancement of the single-mode antenna.
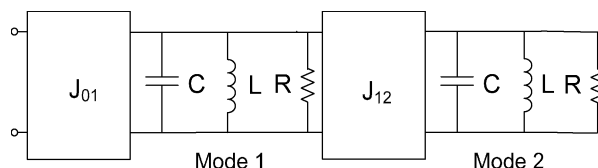
Fig. 1. Dual-mode antenna equivalent circuit.

II. THEORY AND DESIGN ANALYSIS

In the previous dual-mode design [10], the input feeds into one mode, which is then coupled to the orthogonal mode via a discontinuity (notch) in the structure. This discontinuity is located at an angle of 135° from the feed line [9], [11], [12]. The theory related to this design can be clearly illustrated in terms of the equivalent circuit shown in Fig. 1. Here the admittance inverters J_{01} and J_{12} are networks commonly used in filter design, with transfer matrix T given by (1) as follows:

$$[T] = \begin{bmatrix} 0 & jJ_{01} \\ j/J_{01} & 0 \end{bmatrix}. \qquad (1)$$

The equivalent circuit resistors represent the radiation resistance of each mode, the capacitors and inductors represent the resonant modes of the antenna. The admittance inverters J_{01} and J_{12} represent the input matching to the antenna and the coupling between the two modes, respectively. By correct choice of J_{01} and J_{12}, the input return-loss bandwidth can be maximized. The theory of the coupling matrix in filter prototypes is further explained in [12] and [13].

A. Quadruple-Mode Antenna Basic Theory

The dual-mode design approach can be extended by stacking two dual-mode antennas, as shown in Fig. 2. Here, the arrows represent the two orthogonal resonant modes on each layer (1 and 2 on the bottom layer and 3 and 4 on the top layer). The input feeds into mode 1, which is coupled to mode 2 via a discontinuity. Couplings may then exist between all four modes and, therefore, all those couplings must be analyzed.

The generalized equivalent circuit of the antenna is shown in Fig. 3, denormalized to a low-pass prototype form.

In reality, electromagnetic couplings between the patches should only occur between modes 1–4 and 2–3. The couplings between modes 1–3 and 2–4 can be assumed zero at this stage.
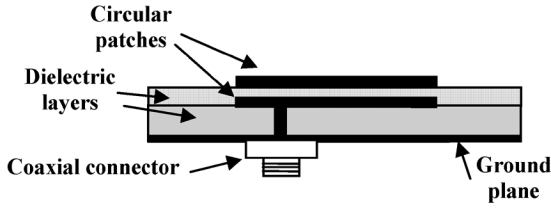
Fig. 2. (a) Quad-mode patch antenna physical design (side view). (b) Four resonant modes in the quadruple mode patch antenna.
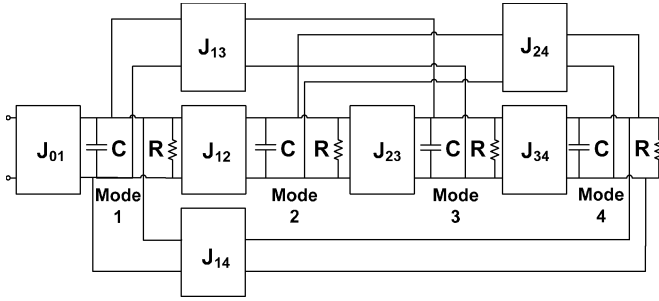

Fig. 3. Quad-mode circular microstrip patch antenna low-pass prototype considering all the possible electromagnetic couplings between the four modes in the physical model.
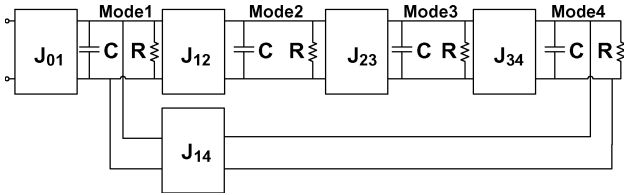

Fig. 4. Quad-mode circular microstrip patch antenna low-pass prototype.

Considering these assumptions, the circuit in Fig. 3 reduces to the one in Fig. 4;

In Section II-B, it is shown how the prototype networks in Figs. 3 and 4 can be derived analytically, reaching an equivalent circuit for the antenna with the correct coupling values.

B. Mathematical Transformations

Fig. 5 shows a fourth-order low-pass ladder network, where all the capacitances and resistances are normalized to unity. The
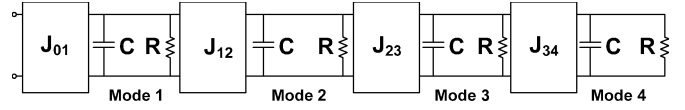

Fig. 5. Fourth-order low-pass ladder network ($N = 4$ and $R = C = 1$).

expression for the reflection coefficient $S_{11}(p)$ of this network can be derived using circuit analysis techniques in [12], which is shown in (2) at the bottom of this page.

The correct coupling values $J_{01} - J_{34}$ can be determined by designing the network to have a quasi-equiripple return-loss characteristics using techniques described in [12] and [14]. The return-loss function for a low-pass equiripple prototype resonator of order r is shown in (3) [14] as follows:

$$S_{11(p)} = \prod_{r=1}^{n} \frac{p - j\omega_r}{p - j\omega_r + \frac{2}{Q}}, \qquad \text{where } Q = \omega CR. \quad (3)$$

For the quadruple-mode antenna being considered here, n is equal to 4, Q is equal to 1 (assuming $R = C = 1$), and using optimization techniques, the ω_r value for $r = 1 \rightarrow n$ can be found to achieve an equiripple response. Therefore, with a 6-dB return-loss ripple level (which is typical for handset antennas), the expression of the reflection coefficient $S_{11}(p)$ is given by

$$S_{11}(p) = \frac{p^4 + 46.4425p^2 + 201.3561}{p^4 + 8p^3 + 70.4425p^2 + 217.77p + 403.1261} \quad (4)$$

(with $\omega_1 = \pm 2.2$ s^{-1} and $\omega_2 = \pm 6.25$ s^{-1}).

By equating the coefficients of (2) and (4), the coupling values ($J_{01} - J_{34}$) can be obtained, which are

$$J_{01} = 2 \quad J_{12} = 5.296 \quad J_{23} = 3.898 \quad J_{34} = 2.976. \quad (5)$$

The network in Fig. 5 is simulated using these values and the response is shown in Fig. 6. The coupling values in (5) show a 6-dB bandwidth increase compared to a single-mode design of 5.7 times.

However, the actual equivalent circuit of the practical antenna includes nonadjacent couplings between modes, as shown in Fig. 3.

$$S_{11}(p) = \frac{\begin{array}{l} p^4 + p^3 \left(4 - J_{01}^2\right) + p^2 \left(6 - 3J_{01}^2 + J_{12}^2 + J_{23}^2 + J_{34}^2\right) \\ + p \left(4 - 3J_{01}^2 + 2J_{12}^2 + 2J_{23}^2 + 2J_{34}^2 - J_{01}^2 J_{34}^2 - J_{01}^2 J_{23}^2\right) \\ + \left(1 - J_{01}^2 + J_{12}^2 + J_{23}^2 + J_{34}^2 + J_{12}^2 J_{34}^2 - J_{01}^2 J_{34}^2 - J_{01}^2 J_{23}^2\right) \end{array}}{\begin{array}{l} p^4 + p^3 \left(4 + J_{01}^2\right) + p^2 \left(6 + 3J_{01}^2 + J_{12}^2 + J_{23}^2 + J_{34}^2\right) \\ + p \left(4 + 3J_{01}^2 + 2J_{12}^2 + 2J_{23}^2 + 2J_{34}^2 - J_{01}^2 J_{34}^2 - J_{01}^2 J_{23}^2\right) \\ + \left(1 + J_{01}^2 + J_{12}^2 + J_{23}^2 + J_{34}^2 + J_{12}^2 J_{34}^2 + J_{01}^2 J_{34}^2 + J_{01}^2 J_{23}^2\right) \end{array}} \quad (2)$$
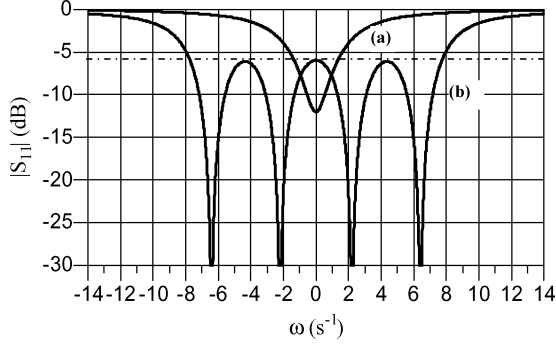
Fig. 6. Simulation results of the equivalent low-pass circuit prototype of: (a) single-mode antenna and (b) quad-mode antenna.

The admittance matrix of the low-pass prototype in Fig. 5 is

$$[y] = \begin{bmatrix} 0 & jJ_{01} & 0 & 0 & 0 \\ jJ_{01} & 1+p & jJ_{12} & 0 & 0 \\ 0 & jJ_{12} & 1+p & jJ_{23} & 0 \\ 0 & 0 & jJ_{23} & 1+p & jJ_{34} \\ 0 & 0 & 0 & jJ_{34} & 1+p \end{bmatrix} \qquad (6)$$

or

$$[y] = \begin{bmatrix} 0 & 0 & 0 & 0 & 0 \\ 0 & 1+p & 0 & 0 & 0 \\ 0 & 0 & 1+p & 0 & 0 \\ 0 & 0 & 0 & 1+p & 0 \\ 0 & 0 & 0 & 0 & 1+p \end{bmatrix} \\ + \begin{bmatrix} 0 & jJ_{01} & 0 & 0 & 0 \\ jJ_{01} & 0 & jJ_{12} & 0 & 0 \\ 0 & jJ_{12} & 0 & jJ_{23} & 0 \\ 0 & 0 & jJ_{23} & 0 & jJ_{34} \\ 0 & 0 & 0 & jJ_{34} & 0 \end{bmatrix} \qquad (7)$$

where the second part of (7) is known as the coupling matrix $j[J]$ [12], [13].

This coupling matrix may be pre- and post-multiplied by rotational matrices without altering the input reflection coefficient response, provided that these matrices do not operate on the first row and column. This process is known as matrix rotation [12]. If 2–4 and 2–3 rotations are applied to the coupling matrix $[J]$,

the result is shown as follows in (8), (9), and (11), and shown in (10) at the bottom of this page:

$$[J_{2\times4}] \rightarrow [\mathrm{T}_{24}]^{-1} \begin{bmatrix} 0 & J_{01} & 0 & 0 & 0 \\ J_{01} & 0 & J_{12} & 0 & 0 \\ 0 & J_{12} & 0 & J_{23} & 0 \\ 0 & 0 & J_{23} & 0 & J_{34} \\ 0 & 0 & 0 & J_{34} & 0 \end{bmatrix} [\mathrm{T}_{24}] \quad (8)$$

$$[J] \rightarrow [\mathrm{T}_{23}]^{-1}[J_{2\times4}][\mathrm{T}_{23}] \qquad (9)$$

where

$$[\mathrm{T}_{24}] = \begin{bmatrix} 0 & 0 & 0 & 0 & 0 \\ 0 & 0 & 0 & 0 & 0 \\ 0 & 0 & C_{2\times4} & 0 & S_{2\times4} \\ 0 & 0 & 0 & 0 & 0 \\ 0 & 0 & -S_{2\times4} & 0 & C_{2\times4} \end{bmatrix}$$

$$[\mathrm{T}_{23}] = \begin{bmatrix} 0 & 0 & 0 & 0 & 0 \\ 0 & 0 & 0 & 0 & 0 \\ 0 & 0 & C_{2\times3} & S_{2\times3} & 0 \\ 0 & 0 & -S_{2\times3} & C_{2\times3} & 0 \\ 0 & 0 & 0 & 0 & 0 \end{bmatrix}$$

with the final result shown in (10), where

$$C_{2\times4} = \cos(\theta_{2\times4}) \text{ and } S_{2\times4} = \sin(\theta_{2\times4})$$
$$C_{2\times3} = \cos(\theta_{2\times3}) \text{ and } S_{2\times3} = \sin(\theta_{2\times3}). \qquad (11)$$

This result takes into account all the possible electromagnetic couplings in the physical structure in Fig. 2. The coupling between modes 1–3, 1–4, 2–3, and 2–4 are now nonzero. This matrix describes the circuit in Fig. 3.

It can be assumed that the coupling between modes 2–3 and 1–4 are equal, as are the cross couplings between modes 2–4 and 1–3. Hence, θ_{23} and θ_{24} can be found by equating the values for the coupling between modes 2–3 and 1–4, and coupling between modes 1–3 and 2–4 in (10). This will force the cross couplings J_{13} and J_{24} to zero and equalize the adjacent couplings J_{14} and J_{23} to reach a circuit similar to the one in Fig. 4, thus,

$$j \cdot S_{2\times3} \cdot C_{2\times4}J_{12} = -j \cdot S_{2\times3} \cdot (S_{2\times4} \cdot J_{23} + C_{2\times4} \cdot J_{34}) \qquad (12)$$

$$j \cdot S_{2\times4} \cdot J_{12} = -j \cdot S_{2\times3}^2 \cdot (C_{2\times4} \cdot J_{23} - S_{2\times4} \cdot J_{34}) \\ + j \cdot C_{2\times3}^2 \cdot (C_{2\times4} \cdot J_{23} - S_{2\times4} \cdot J_{34}). \qquad (13)$$

$$[J] \rightarrow \begin{bmatrix} 0 & J_{01} & 0 & 0 & 0 \\ J_{01} & 0 & C_{2\times3}\cdot C_{2\times4}J_{12} & S_{2\times3}\cdot C_{2\times4}J_{12} & S_{2\times4}\cdot J_{12} \\ 0 & C_{2\times3}\cdot C_{2\times4}\cdot J_{12} & -2\cdot S_{2\times3}\cdot C_{2\times3}(C_{2\times4}\cdot J_{23}-S_{2\times4}\cdot J_{34}) & -S_{2\times3}^2\cdot(C_{2\times4}\cdot J_{23}-S_{2\times4}\cdot J_{34})+C_{2\times3}^2\cdot(C_{2\times4}\cdot J_{23}-S_{2\times4}\cdot J_{34}) & -S_{2\times3}\cdot(S_{2\times4}\cdot J_{23}+C_{2\times4}\cdot J_{34}) \\ 0 & S_{2\times3}\cdot C_{2\times4}\cdot J_{12} & -S_{2\times3}^2\cdot(C_{2\times4}\cdot J_{23}-S_{2\times4}\cdot J_{34})+C_{2\times3}^2\cdot(C_{2\times4}\cdot J_{23}-S_{2\times4}\cdot J_{34}) & 2\cdot S_{2\times3}\cdot C_{2\times3}\cdot(C_{2\times4}\cdot J_{23}-S_{2\times4}\cdot J_{34}) & C_{2\times3}\cdot(S_{2\times4}\cdot J_{23}-C_{2\times4}\cdot J_{34}) \\ 0 & S_{2\times4}\cdot J_{12} & -S_{2\times3}\cdot(S_{2\times4}\cdot J_{23}+C_{2\times4}\cdot J_{34}) & C_{2\times3}\cdot(S_{2\times4}\cdot J_{23}-C_{2\times4}\cdot J_{34}) & 0 \end{bmatrix} \qquad (10)$$

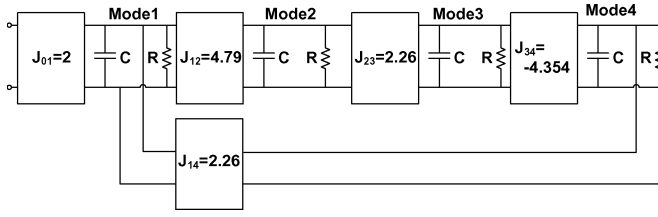Fig. 7. Quad-mode circular microstrip patch antenna low-pass prototype.

Fig. 8   Physical dimensions of the antenna. (a) Bottom layer. (b) Top layer.

The values of $\theta_{2\times3}$ and $\theta_{2\times4}$ that satisfy (12) and (13) are

$$\theta_{2\times3} = \pi \text{ and } \theta_{2\times4} = 0.44029. \tag{14}$$

These values alongside the coupling values found in (5) were used to evaluate $[J]$ in (10) and the result is shown in (15) and depicted in Fig. 7 as follows:

$$[J] \rightarrow \begin{bmatrix} 0 & 2 & 0 & 0 & 0 \\ 2 & 0 & -4.793 & 0 & 2.26 \\ 0 & -4.793 & 0 & 2.26 & 0 \\ 0 & 0 & 2.26 & 0 & -4.354 \\ 0 & 2.26 & 0 & -4.354 & 0 \end{bmatrix}. \tag{15}$$

Here it can be clearly seen that there will definitely be equal couplings between modes 1–4 and 2–3. The other couplings between modes 1–3 are 2–4 are zero, as expected.

III. ELECTROMAGNETIC SIMULATIONS AND MEASURED RESULTS

The resonant frequency of a circular microstrip patch antenna in the dominant TM_{110} mode is given by [15]–[17]

$$f_r = \frac{c \cdot \chi'_{mn}}{2\pi a(\varepsilon r)^{\frac{1}{2}}} \tag{16}$$

where fr is the resonant frequency, χ'_{mn} are the zeros of the Bessel function of order n and equal to 1.8412 for the dominant TM_{110} mode, and a is the radius of the circular patch. The radius of circular microstrip patch antenna is fabricated on Duroid 5880, $\epsilon_r = 2.2$, thickness is 787 mm, and operating at 2 GHz is approximately 30 mm. In designing a quadruple-mode antenna, the most logical procedure is to start with the bottom patch and obtain the correct coupling between the first two modes. For instance, if the circuit in Fig. 7 is simulated with couplings J_{12}, J_{23}, J_{34}, and J_{14} are all reduced to zero, this would leave us with the bottom patch only, and hence, the simulated return loss at the center frequency is -4.4 dB. This result enables us to locate the position of the feed point across the radius of the patch [1] at 17 mm from the center point.

The second step is to introduce the coupling between the first two modes on the bottom patch, i.e., J_{12}. If the circuit in Fig. 7 is simulated with all couplings reduced to zero apart from J_{01} and J_{12}, the result indicates the return-loss bandwidth of modes 1–2 only. The coupling level between them is found to be approximately 3 dB. A notch 6.17×5 mm placed at 135° from the feed line is introduced at the bottom patch, and with the aid of computer simulations, it can be designed to achieve a coupling of 3 dB between modes 1–2 in the same manner as [10].
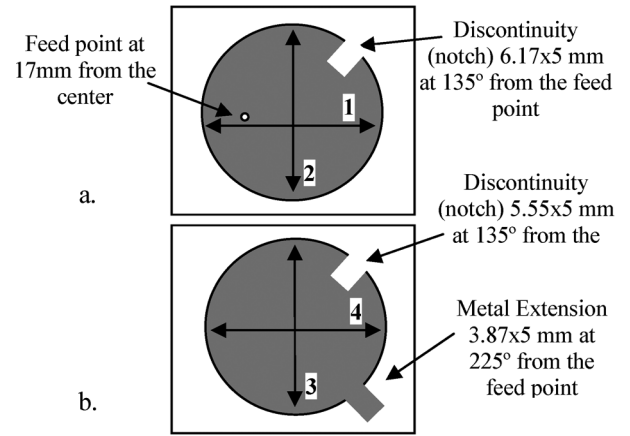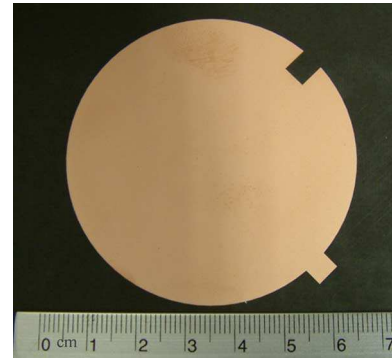

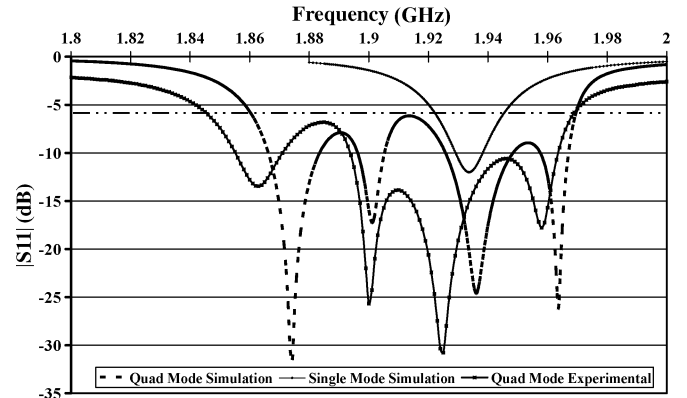Fig. 9. Quade-mode patch antenna prototype (top view).

Fig. 10. Simulation and measured results of the quad-mode antenna design showing 4.2 times wider 6-dB return-loss bandwidth compared to single mode.

At this stage, the bottom patch is now designed. The top patch may now be introduced and the dimensions of the second notch may be evaluated. Three tuning parameters were found useful to achieve the overall maximum 6-dB return-loss bandwidth, these are the thickness of the substrate between the two patches that controls the coupling strength between the two layers, a notch at one mode and a metal extension on the other mode controlling the couplings J_{23} and J_{14}, respectively. By tuning the circuit using computer simulation, a 5.55×5 mm notch is placed at 135° from the feed line on the upper patch and a metal extension
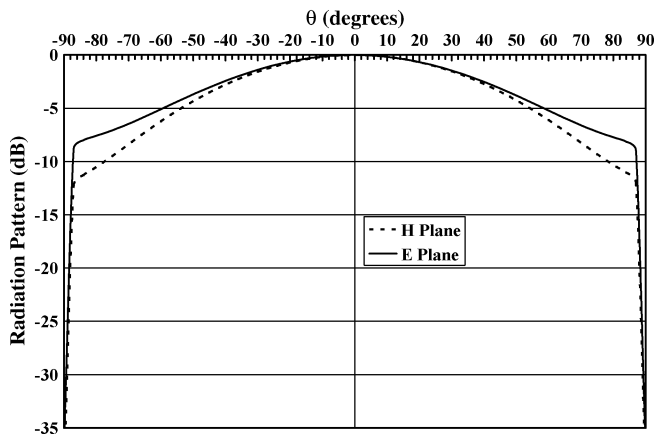
Fig. 11. Far-field radiation pattern of the antenna.

of 3.87 × 5 mm placed at 225° from the feed line on the top patch, where the top substrate thickness is 0.381 mm.

A quadruple-mode antenna (Figs. 8 and 9) has been designed with total thickness of 1.168 mm. Simulated and measured results in Fig. 10 shows a bandwidth increase of over 4.2 times compared to a single mode.

The far-field radiation pattern plot is shown in Fig. 11. This is similar to a single-mode patch antenna.

IV. CONCLUSION

Microstrip patch antennas enjoy many advantages and qualities; however, one major issue is the inherent narrow bandwidth. This paper presents a new approach for the synthesis of a dual-layer quadruple-mode circular microstrip patch antenna. Using matrix rotation techniques normally employed in filter design, the equivalent circuit and coupling values were found. These were then applied to the antenna synthesis, resulting in increasing the return-loss bandwidth by 4.2 times compared to a single-mode design. Circuit and electromagnetic simulations show excellent results, which agree well with the measured results. This is the first time that such an approach of designing antennas as multimode filters has been demonstrated.

ACKNOWLEDGMENT

REFERENCES

[1] R. Garg, *Microstrip Antenna Design Handbook*. Norwood, MA: Artech House, 2001.
[2] G. Sanford, Ball Corporation, Muncie, IN, , "Multiple resonance radio frequency microstrip antenna structure," U.S. 4 070 676, Jan. 24, 1978.
[3] S. A. Long and M. D. Walton, "A dual-frequency stacked circular-disc antenna," *IEEE Trans. Antennas Propag.*, vol. AP-27, no. 2, pp. 270–273, Mar. 1979.
[4] P. S. Hall *et al.*, "Wide bandwidth microstrip antennas for circuit integration," *Electron. Lett.*, vol. 15, pp. 458–460, 1979.
[5] G. Kumar and K. P. Ray, *Broadband Microstrip Antennas*. London, U.K.: Artech House, 2003.
[6] S. Maci and G. B. Gentili, "Dual-frequency patch antennas," *IEEE Antennas Propag. Mag.*, vol. 39, no. 6, pp. 13–20, Dec. 1997.
[7] K. Lee and W. Chen, *Advances in Microstrip and Printed Antennas*. New York: Wiley, 1997.
[8] D. M. Pozar and D. Schaubert, *Microstrip Antennas*. New York: Wiley, 1995.
[9] K. Chang, *Microwave Ring Circuits and Antennas*. New York: Wiley, 1996.
[10] A. I. Abunjaileh, I. C. Hunter, and A. H. Kemp, "Application of dual-mode filter techniques to the broadband matching of microstrip patch antennas," *IET Microw., Antennas. Propag.*, vol. 1, pp. 273–276, 2007.
[11] I. Hunter, "Broad-band matching of antennas using dual-mode radiators," presented at the 33rd Eur. Microw. Conf., 2003.
[12] I. Hunter, *Theory and Design of Microwave Filters*. London, U.K.: IEE Press, 2001.
[13] H. C. Bell, "The coupling matrix in low-pass prototype filters," *IEEE Micro*, vol. 8, no. 2, pp. 70–76, Apr. 2007.
[14] J. D. Rhodes, Filtronic Comtek PLC, West Yorkshire, U.K., "Microwave reflection filter including a ladder network of resonators having progressively smaller Q values," U.S. Patent 5 781 084, 1998, 12 pp.
[15] I. J. Bahl and P. Bhartia, *Microstrip Antennas*. Norwood, MA: Artech House, 1980.
[16] C. A. Balanis, *Antenna Theory: Analysis and Design*, 2nd ed. New York: Wiley, 1997.
[17] N. Kumprasert and W. Kiranon, "Simple and accurate formula for the resonant frequency of the circular microstrip disk antenna," *IEEE Trans. Antennas Propag.*, vol. 43, no. 11, pp. 1331–1333, Nov. 1995.

Alaa I. Abunjaileh (S'07) was born in Amman, Jordan. He received the B.Eng. (first-class Hons) degree in electronic and communications engineering from The University of Leeds, Leeds, U.K., in 2004, and is currently working toward the Ph.D. degree at The University of Leeds.

He is currently a Research and Teaching Assistant with The University of Leeds. During his undergraduate studies, he spent almost a year in industry as an Electronic and Communications Engineer with Siddal and Hilton (in the U.K.) and overseas with SITA International. He has also been a Research Assistant involved with joint projects between The University of Leeds, Rio Tinto, DTI UK, TDK, and Wansfell Design Ltd.

Ian C. Hunter (M'82–SM'94–F'07) received the B.Sc. (first-class Hons) and Ph.D. degrees from The University of Leeds, Leeds, U.K., in 1978 and 1981, both in electrical engineering.

He has worked in industry for Aercom Industries Inc., Sunnyvale, CA, KW Engineering, Oakland, CA, and Filtronic Components Ltd., Leeds, U.K., during which time he developed broadband microwave filters for electronic warfare (EW) applications. From 1995 to 2001, he was with Filtronic Comtek, where he was involved with advanced filters for cellular radio. He is currently a Professor with the School of Electronic and Electrical Engineering, The University of Leeds, where he teaches circuit theory, electromagnetism, and microwave engineering. He authored *Theory and Design of Microwave Filters* (IEE Press, 2001). His research includes linear and nonlinear microwave filters. He also investigates applications of microwaves in biology.

Andrew H. Kemp received the B.Sc. degree in electronics from the University of York, York, U.K. in 1984, and the Ph.D. degree from the University of Hull, Hull, U.K., in 1991.

He worked in industry while earning his doctoral degree. Since 1998, he has been with The University of Leeds, Leeds, U.K., where he is currently a Senior Lecturer. His research interests include statistical characterization of multipath propagation environments, wireless sensor network (WSN) with localization, and investigating Internet quality of service issues.

Dr. Kemp is a member of the Institution of Electrical Engineers (IEE), U.K. He is a Fellow of the Higher Education Academy of the U.K.